



# Use Of Olivine For The Production Of MgO-SiO<sub>2</sub> Binders

Scott Allan Nye<sup>1\*</sup>, Shah Vineet<sup>1</sup>, Oze Christopher<sup>2</sup>, Shanks Barnaby<sup>3</sup> and Cheeseman Chris<sup>3</sup>

<sup>1</sup>Department of Civil and Natural Resources Engineering, University of Canterbury, Christchurch, New Zealand, <sup>2</sup>Geology Department, Occidental College, Los Angeles, CA, United States, <sup>3</sup>Department of Civil and Environmental Engineering, Imperial College London, London, United Kingdom

The potential for using MgO and SiO<sub>2</sub>, recovered from olivine, was investigated for use as a cementitious binder system. The MgO to SiO<sub>2</sub> proportion for the binder was fixed at 1:1. The nature of the hydration products were characterized using a variety of techniques including isothermal calorimetry, XRD, FTIR, and SEM. The primary binding component of the paste was determined to be magnesium silicate hydrate (M-S-H). The recovered silica exhibited faster reactivity compared to commercially available silica fume. Compressive strengths in excess of 20 MPa were obtained using the materials recovered from olivine.

**Keywords:** olivine, acid digestion, electrolysis, MgO, hydration, compressive strength

## OPEN ACCESS

### Edited by:

Brant Walkley,  
The University of Sheffield,  
United Kingdom

### Reviewed by:

Mohammad M. Karimi,  
Tarbiat Modares University, Iran  
Hajime Kinoshita,  
The University of Sheffield,  
United Kingdom

### \*Correspondence:

Scott Allan Nye  
allan.scott@canterbury.ac.nz

### Specialty section:

This article was submitted to  
Sustainable Design and Construction,  
a section of the journal  
Frontiers in Built Environment

**Received:** 10 December 2020

**Accepted:** 29 April 2021

**Published:** 21 May 2021

### Citation:

Allan Nye S, Vineet S, Christopher O,  
Barnaby S and Chris C (2021) Use Of  
Olivine For The Production Of MgO-  
SiO<sub>2</sub> Binders.  
Front. Built Environ. 7:640243.  
doi: 10.3389/fbuil.2021.640243

## INTRODUCTION

Considerable research has been conducted investigating the potential use of MgO-SiO<sub>2</sub> binder systems (Zhang et al., 2011, Zhang et al., 2014; Tran and Scott, 2017; Shah and Scott, 2019; Bhagath Singh et al., 2020). The poorly crystalline magnesium silicate hydrates (M-S-H) formed by the reaction between MgO and reactive silica sources provides binding characteristics similar to calcium silicate hydrates (C-S-H) formed in the pozzolanic reaction of supplementary cementitious materials with calcium hydroxide. The structural form of the two are somewhat different with C-S-H typically having a dreierketten structure whereas M-S-H has a layered silicate structure similar to clay minerals (Bernard et al., 2017). The specific characteristics of the M-S-H is affected by the physical and chemical properties of the constituent raw materials (MgO and SiO<sub>2</sub>), mix design and curing conditions (Jia et al., 2017; Tran and Scott, 2017; Abdel-Gawwad et al., 2018; Li et al., 2018; Sonat and Unluer, 2019; Dhakal et al., 2021; Shah and Scott, 2021b). MgO-SiO<sub>2</sub> binders have shown potential for applications in: waste immobilization/encapsulation where a lower pH (< 10.5) environment is required; as refractory castables because of high melting temperature; and as building materials due to excellent mechanical properties (Zhang et al., 2012, Zhang et al., 2014; Walling et al., 2015; Walling and Provis, 2016; Tran and Scott, 2017).

The MgO required for such a binder system is typically obtained from the calcination of magnesite (MgCO<sub>3</sub>) in a temperature range of 700–1000°C. The reserves of magnesite are sporadically distributed around the world with the majority of the deposits located in a small numbers of countries. The identified total reserves of magnesite is around 13 billion tonnes while the annual global production of Portland cement (PC) is ~3 billion tonnes (Shand, 2006; UN Environment et al., 2018). If MgO-SiO<sub>2</sub> binder are to be used on a large scale and as a potential substitute for PC, it is essential to look for alternate sources of magnesium oxide. In addition, most of the studies investigated MgO-SiO<sub>2</sub> binders, use either silica fume or micro-silica as the reactive SiO<sub>2</sub> source (Jin and Al-Tabbaa, 2014; Zhang et al., 2014; Tran and Scott, 2017). The quantities of these SiO<sub>2</sub> sources are limited and most are already being used in the conventional cement industry. The use of fly ash and slag alongside MgO has also been reported. However, the low reactivity of fly ash and the presence of CaO in slag limits the effectiveness of the binder (Vandeperre et al., 2008; Jia

et al., 2017; Tran, 2019). Alternatively, the use of calcined clay and rice husk ash as SiO<sub>2</sub> source has also been reported (Sonat and Unluer, 2019; Shah and Scott, 2021b, 2021a).

Ultramafic magnesium silicate minerals are abundantly available worldwide with reserves of over 10 trillion tonnes (Pacheco-Torgal et al., 2018). The use of magnesium silicate minerals has been proposed as one potential option for carbon sequestration. The sequestration of CO<sub>2</sub> using magnesium silicate minerals and production of MgO, as a potential commercial binder, is currently limited by the availability of an energy efficient industrial process (Matter and Kelemen, 2009; Sanna et al., 2013, 2014; Vlasopoulos and Cheeseman, 2013; Walling and Provis, 2016; Gartner and Sui, 2018; UN Environment et al., 2018). Magnesium silicate minerals could however serve as an ideal feedstock to produce MgO-SiO<sub>2</sub> binders, if the MgO and SiO<sub>2</sub> could be extracted efficiently. Unlike magnesite for MgO or limestone for PC that releases chemical CO<sub>2</sub> in raw materials during calcination, magnesium silicate minerals do not have any inherent CO<sub>2</sub> associated with them. Therefore, it possesses the potential to be a truly carbon negative binder. The cement industry accounts for approximately 8% of global CO<sub>2</sub> emissions (Kajaste and Hurme, 2016; Gartner and Sui, 2018), and the successful development of a method to extract oxides from magnesium silicate minerals would bring significant benefits.

The authors have recently demonstrated an energy-efficient method that could be used to separate MgO and SiO<sub>2</sub> from olivine, a form of magnesium silicate minerals (Scott et al., 2021). The process uses a combination of acid digestion and electrolysis techniques for the successful extraction of oxides. The binding characteristics of the extracted oxides however have not been investigated yet. In this proof of concept study, the efficacy of the oxides extracted from olivine used to produce a MgO-SiO<sub>2</sub> binder system are investigated. The MgO-SiO<sub>2</sub> binder characteristics are determined using a range of techniques including isothermal calorimetry, XRD, FTIR, and compressive strength.

## EXTRACTION METHOD

Ground olivine with an average particle size of 30 μm was used in the study. The olivine was mixed with 2 M HCl in a ratio of 1:10 (% W/V) in a beaker and placed on a hot plate at a temperature of 60°C and stirred continuously. After 2 h of digestion, the solution was left to stand for one hour and subsequently decanted to remove any unreacted olivine. The decanted solution primarily consists of silica, magnesium, iron, and chloride ions as confirmed by ICP-MS testing. The components were individually separated by increasing the pH in steps. Firstly, magnesium hydroxide (0.2% w/v) was added in the decanted solution to raise the pH to >3.1. The increase in pH results in condensation and polymerization of silicic acid (Si(OH)<sub>4</sub>) forming silica gel (Besbes et al., 2009). The silica formed through this process is analogous to the sol-gel method used to extract nano-silica from sodium metasilicate (Gorrepati et al., 2010; Katouezadeh et al., 2020). The polymerized silica was filtered out and repeatedly washed with water to remove any

excess acid or chloride salts. Thereafter, 2 M NaOH was added in the filtered solution to raise the pH to 6.5 to 7. The increase in pH leads to precipitation of iron hydroxide, which was subsequently removed through either filtration or centrifugation. The filtered solution was electrolyzed to form magnesium hydroxide at the cathode. Approximately 35 g of Mg(OH)<sub>2</sub> was obtained from 100 g of olivine, of which 1 g was added during the silica precipitation stage. Hydrogen gas (cathode) and chlorine gas (anode) could be recovered to produce HCl for reuse in the digestion process. The developed process could result in significant CO<sub>2</sub> savings, even if fossil fuels were used as the energy source, as no chemical CO<sub>2</sub> is released in the process. In the final stage of the binder component production, the Mg(OH)<sub>2</sub> obtained from electrolysis was calcined at 500°C for 1 h to produce MgO.

The silica (RS) and MgO (RM) recovered from olivine using the extraction procedure was assessed for its binder characteristics. The performance of MgO-SiO<sub>2</sub> binder prepared from the recovered material was compared with commercially available MgO and silica fume using: isothermal calorimetry, XRD, FTIR, and SEM.

## MATERIALS AND EXPERIMENTS

Olivine used for extraction of MgO and SiO<sub>2</sub> was sourced from Red Hills, New Zealand. Commercial MgO (CM) and Silica fume (SF) were obtained from Sibelco Australia and Sika New Zealand, respectively. The chemical composition of the olivine, recovered and commercial MgO and SiO<sub>2</sub> are given in **Table 1**. The high LOI of recovered silica is associated with the loss of water molecules trapped in polymerized silica network (Raza et al., 2018). **Figure 1** shows the XRD patterns of the raw materials. The recovered and commercial MgO show similar characteristics with minor peaks of uncalcined brucite. The recovered silica has an amorphous hump analogous to the commercial silica fume with minor impurities of unreacted olivine (lizardite and forsterite).

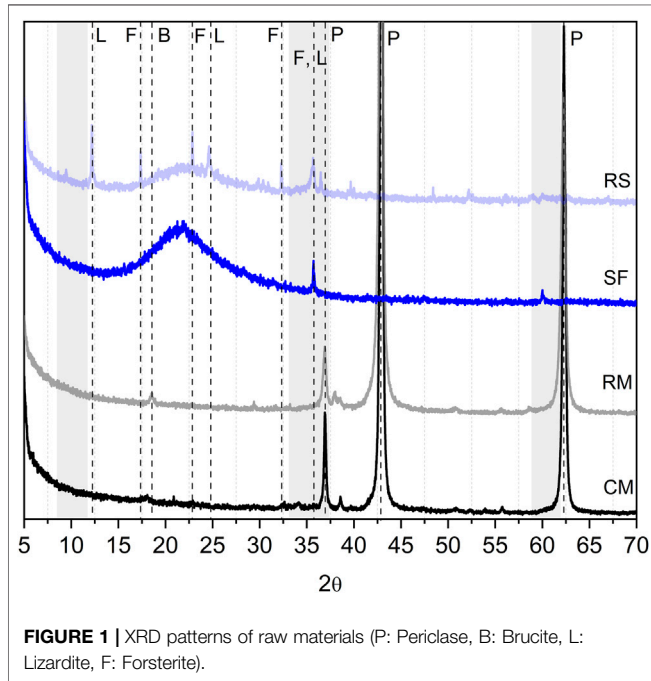
The MgO-SiO<sub>2</sub> binders were prepared by mixing MgO and SiO<sub>2</sub> at 1:1 ratio by mass. The composition of the mixes investigated are presented in **Table 2**. Paste samples were prepared at a water to binder (w/b) ratio of one. This produced mixes with consistent workability and allowed the intrinsic hydration behaviour of the materials to be determined without the influence of any external agents such as superplasticiser.

Approximately 20 g of paste sample was placed in an isothermal calorimeter maintained at 20°C (Calmetrix I-Cal Flex) to measure the heat evolved during hydration in different mixes. The heat values were recorded every 5 min for 72 h. The remaining paste was poured into PVC vials (Diameter 20 mm, Height 100 mm) and cured until the age of testing in a room maintained at 20°C.

Paste samples were taken from the PVC vials after 3, 7, and 28 days for hydration study. The samples were subsequently stored in isopropanol for 7 days to arrest hydration followed by 3 days vacuum drying. The dried samples were ground with a mortar and pestle and used for further analysis. XRD scans were

**TABLE 1** | Chemical composition of raw materials (%/100 g).

%	CM	RM	SF	RS
SiO <sub>2</sub>	2.11	0.19	94.85	63.18
Al <sub>2</sub> O <sub>3</sub>	0.15	0.16	0.57	0.23
Fe <sub>2</sub> O <sub>3</sub>	0.35	11.45	0.33	4.65
CaO	2.8	0.5	0.27	0.57
MgO	84.16	81.66	0.47	13.92
Na <sub>2</sub> O	<0.01	<0.01	0.33	0.03
K <sub>2</sub> O	<0.01	<0.01	0.76	0.06
LOI	10.66	5.63	1.94	16.37
SSA (m <sup>2</sup> /g)	37	23	17	93



carried out in a range of 5 to 70° using Rigaku SmartLab Diffractometer (40 kV, 30 mA) installed with CuKα radiation. The FTIR spectra were obtained in the range of 4000–400 cm<sup>-1</sup> with a resolution of 4 cm<sup>-1</sup> using Bruker Spectrometer Alpha II. The spectrum obtained was based on an average of 25 scans. The morphology of hydration products of the different mixes at 28 days were characterized using scanning electron microscopy. The vacuum dried fractured samples were coated with carbon prior to imaging using a JEOL 6400 in secondary electron mode with an accelerating voltage of 15 kV.

**TABLE 2** | Mix design proportion.

Notation	Commercial MgO	Silica Fume	Recovered MgO	Recovered Silica
CM-SF	0.50	0.50	-	-
RM-SF	-	0.50	0.50	-
CM-RS	0.50	-	-	0.50
RM-RS	-	-	0.50	0.50

Mortar samples were also prepared for the mixes to determine compressive strength. A binder to sand ratio of 1:3 was kept constant for all the mixes. The recovered materials were found to have a very high water demand similar to silica fume. The water to binder ratio and superplasticizer addition therefore was varied to obtain consistent spread, using the drop table, of approximately 110 ± 10 mm between the mixes, similar to ASTM C109, (2010). 50 × 50 × 50 mm cube samples were cast and placed in an environmental controlled room maintained at a temperature of 20°C and 60% relative humidity for 24 h. The samples were then wrapped in plastic and stored at 20°C until the age of testing.

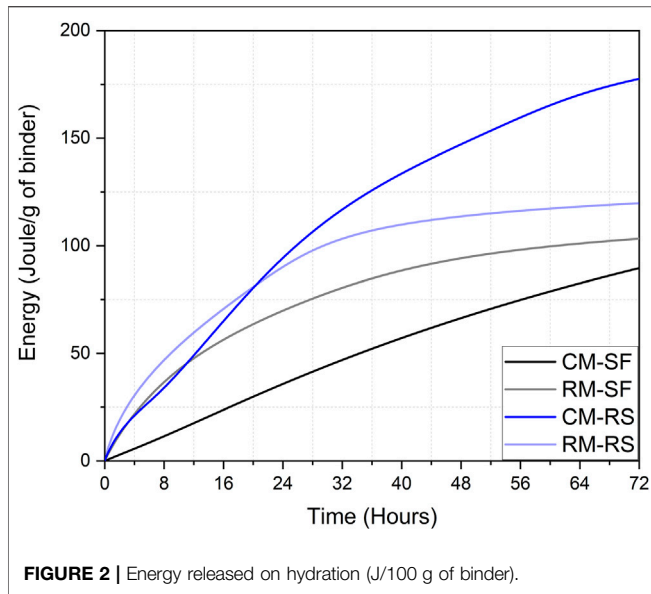
## RESULTS AND DISCUSSION

### Heat Evolution

**Figure 2** shows the cumulative heat evolved from the hydration reaction of different mixes over a period of 72 h measured using isothermal calorimetry. The amount of heat released gives an indication of the extent of reaction between MgO and SiO<sub>2</sub>. A distinct variation in the peak heat evolved and rate of heat evolution can be observed between mixes. Both the mixes with recovered silica (RS) showed a faster and higher heat of hydration compared to silica fume (SF) mixes. The total heat released for CM-SF at the end of 72 h was less than the heat evolved from CM-RS mix in 24 h. This suggests a significantly higher reactivity associated with RS as compared to SF. The RM-RS mix also had a higher total than the RM-SF mix, although the difference was not as great as observed between the CM-RS and CM-SF mixes. The efficacy of recovered MgO (RM) was also compared with the commercial MgO (CM). The heat released in RM-SF mix was consistently higher than CM-SF mix throughout the testing. Whilst the total heat evolved in RM-RS, mix was lower than CM-RS mix, it was more than the commercial CM-SF mix. The results show interesting behavior of the materials recovered from olivine in MgO-SiO<sub>2</sub> binder formulation.

### Hydration Products Qualitative XRD Analysis

The XRD scans of 7 days hydrated samples is shown in **Figure 3**. Prominent peaks corresponding to brucite, formed on the hydration of MgO, are visible in all the mixes. Although, a distinct difference could be observed between the intensity of peaks in SF and RS mixes. The lower or subdued intensity of the brucite peaks in RS mixes indicates a rapid reaction of RS with brucite to form M-S-H. Broad peaks indicative of amorphous M-S-H (represented by grey bands in **Figure 3**) were evident in



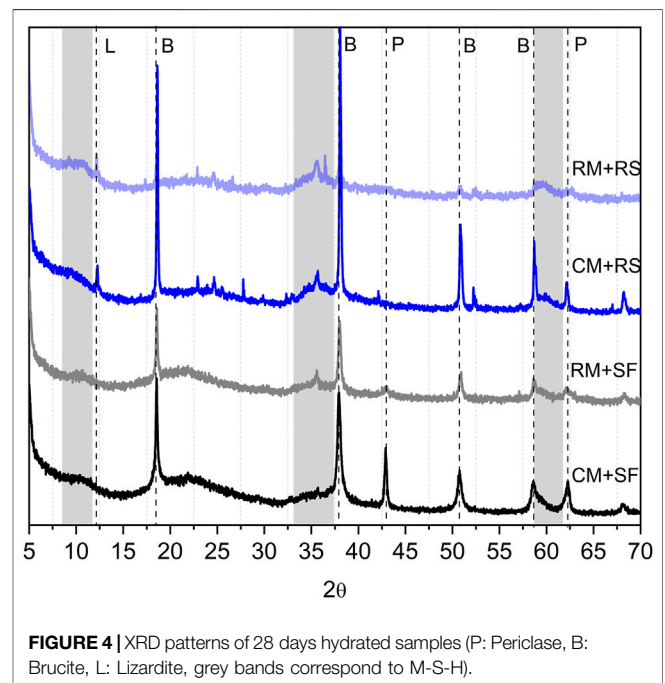
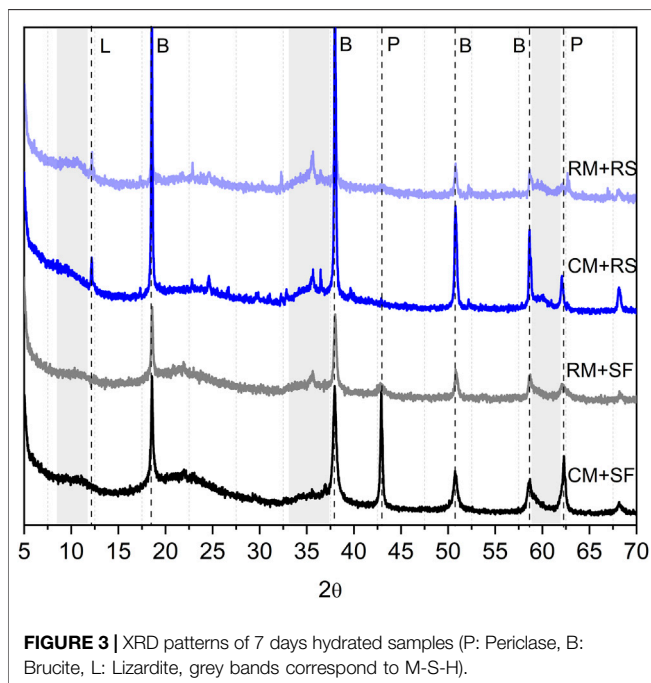
the recovered silica mixes confirming the above postulation (Tonelli et al., 2016; Tran and Scott, 2017; Zhang et al., 2018). The observations are in line with the isothermal calorimetry results, which also showed the highest energy for RS mixes. The higher reactivity of RS is primarily attributed to a high specific surface area. Studies have reported the silica recovered through the sol-gel method is amorphous in nature and possess characteristics of nano-silica (Liefink and Geus, 1998; Gorrepati et al., 2010; Rahman and Padavettan, 2012). The CM-SF mix displays the highest intensity of unreacted MgO peaks of all the mixes suggesting an overall lower degree of hydration. The slower reaction of SF to form M-S-H in the

CM-SF mix may keep the pore solution saturated with magnesium ions, which might slow down the further dissolution of MgO. In the case of the CM-RS mix, the consumption of brucite by RS would create a need for more magnesium ions in the pore solution, which in turn prompts the further dissolution of MgO. This concept is verified from the absence of unreacted MgO peak in CM-RS mix and presence of any observable M-S-H peaks in CM-SF mix. The miniscule peak of unreacted MgO in RM-SF mix suggests a faster dissolution of RM as compared to CM consistent with higher heat evolution in calorimetry. In addition, the lower peak intensities of brucite and more prominent broad peak corresponding to M-S-H in the RM-SF mix suggests a faster reaction of the brucite with silica to form M-S-H in the binder system. This is an interesting observation, which needs further investigation.

**Figure 4** shows the XRD patterns of 28 days hydrated samples. With the increase in the hydration age, the broad peaks corresponding to M-S-H are even more evident particularly in the RM-RS mix with no residual brucite or MgO peaks. Even for the RM-SF mix, the M-S-H peaks are noticeable at 28 days as compared to CM-SF mix where the M-S-H peaks are still not clear. This observation confirms that the materials recovered from olivine could be effectively used to produce MgO-SiO<sub>2</sub> binder. The presence of peaks corresponding to brucite in all the mixes (except RM-RS) indicates the reaction was incomplete and would continue to undergo a transition with time.

### FTIR Analysis

The FTIR spectra of 7 and 28 days hydrated samples are shown in **Figures 5, 6**, respectively. The band at ~3700 and ~1650 cm<sup>-1</sup> are associated with asymmetrical stretching and bending vibrations of O-H bonds, respectively, indicating presence of brucite (Tonelli et al., 2016; Bernard et al., 2019). This confirms that



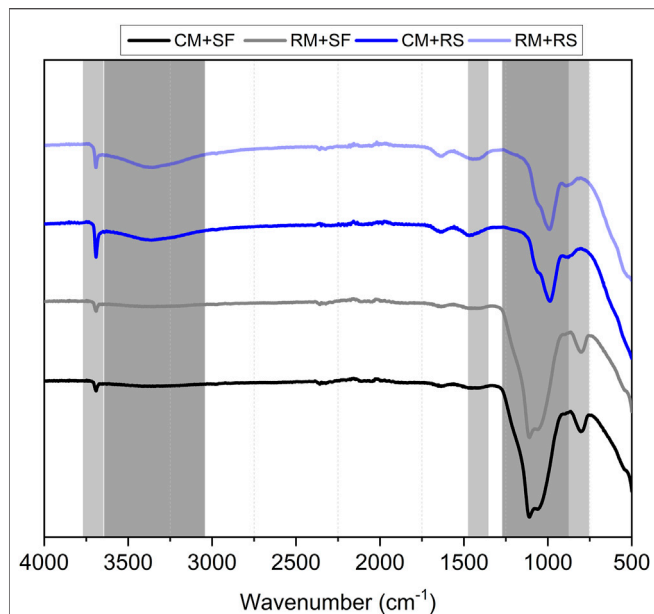


FIGURE 5 | FTIR spectra of 7 days hydrated samples.

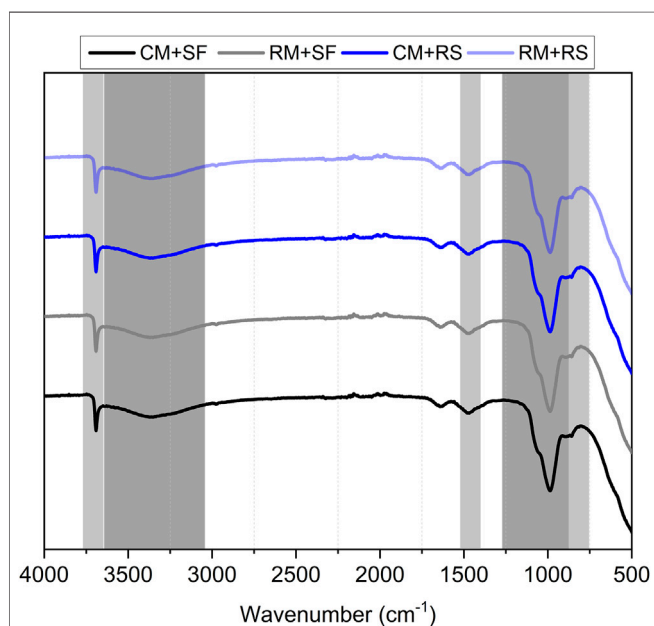


FIGURE 6 | FTIR spectra of 28 days hydrated samples.

the recovered MgO from olivine is reactive and forms brucite similar to commercial MgO. The broad band between  $\sim 3600$  and  $\sim 3200$   $\text{cm}^{-1}$  is characteristically associated with Mg-OH stretching due to the presence of M-S-H phase (Jin and Al-Tabbaa, 2014; Tonelli et al., 2016). A distinctive difference is observed at 7 days between SF and RS mixes in this region. The faster reactivity of RS results in the formation of M-S-H, which can be established from the visible band at  $\sim 3600$  to  $\sim 3200$   $\text{cm}^{-1}$ . However, the absence of this band for SF mixes indicates a lower

overall quantity of M-S-H at 7 days, which is consistent with the XRD results where peaks corresponding to M-S-H were not as definite. With progress in hydration, the band is clearly visible in SF mixes at 28 days confirming the formation of M-S-H. The intense bands in the region of  $\sim 1250$  to  $1000$   $\text{cm}^{-1}$  are associated with Si-O-Si vibrations (Brew and Glasser, 2005; Tonelli et al., 2016; Abdel-Gawwad et al., 2018). The Si-O-Si internal vibrations linked to unreacted silica are generally centered at the higher end of the band. The RS mixes showed a band with the peak centered at  $\sim 1025$   $\text{cm}^{-1}$  corresponding to bending vibrations of Si-O-Si in M-S-H. The SF mixes at 7 days displayed peaks centered at  $\sim 1100$   $\text{cm}^{-1}$ , which are a result of the lower reactivity of the SF to form M-S-H. At 28 days, the peak for SF mixes aligns with RS mixes indicating formation of M-S-H. The disappearance of the peak at  $\sim 800$   $\text{cm}^{-1}$  associated with Si-O-Si internal vibrations of unreacted silica from 7 to 28 days for SF mixes confirms conversion to M-S-H (Abdel-Gawwad et al., 2018; Bhagath Singh et al., 2020). Similar changes corresponding to the peak shift on continued hydration have been reported for MgO-SiO<sub>2</sub> binder system (Brew and Glasser, 2005; Bhagath Singh et al., 2020). The observation of Mg-OH band in RM mixes and change in Si-O-Si band position confirms that the products recovered from olivine have the potential to produce M-S-H on hydration.

## Microstructure

Figure 7 shows the SEM images of 28 days hydrated samples of all the mixes. Homogenous and well-distributed precipitation of hydration products was observed throughout the microstructure. The gel like characteristics of the hydration products in the microstructure suggests the presence of an M-S-H phase. The precipitation of M-S-H surrounding the spherical SF particles can be clearly seen in both the CM and RM mixes. The existence of spherical SF particles implies that the reaction is incomplete and would continue over time. A dense microstructure was observed for the recovered silica mixes. The XRD and FTIR results showed the proportion of M-S-H formed in RS mixes was likely to be higher than in the SF mixes. The similarity between the hydrated microstructures of commercial MgO and SiO<sub>2</sub> and the recovered materials from olivine confirms the ability of olivine to act as the raw materials for the production of MgO-SiO<sub>2</sub> binders.

## Compressive Strength

The compressive strength of mortar samples measured at 3, 7, and 28 days is provided in Table 3. A higher w/b ratio was needed for mixes containing recovered materials due to their higher specific surface area and resulting water demand. Due to the difference in the w/b ratio between the mixes, a direct comparison of the performance is not possible. However, an indication of the material characteristics could be established. The 3 days compressive strength of CM + RS mix was  $\sim 60\%$  higher than CM + SF mix even with a higher w/b ratio. The faster reactivity of the RS as compared to SF could have resulted in the rapid formation of M-S-H, the main strength-imparting phase. This is consistent with the calorimetry results where a higher total heat was observed in CM + RS mix as compared to CM + SF mix. Higher compressive strengths were also observed even after

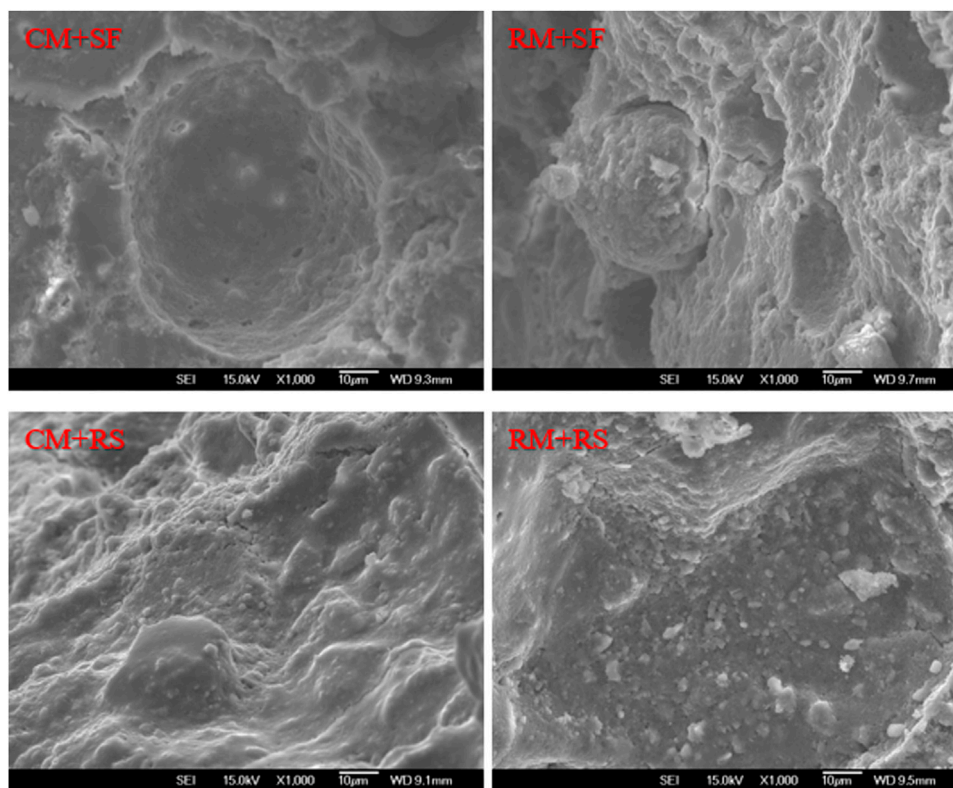


FIGURE 7 | SEM images of 28 days hydrated samples.

TABLE 3 | Summary of compressive strength (MPa) of mixes.

	CM-SF (W/B: 0.50)	CM-RS (W/B: 0.58)	RM-RS (W/B: 0.75)
3 Days	13.7	21.9	16.5
7 Days	30.1	31.4	21.6
28 Days	49.1	36.0	22.0

7 days. The XRD and FTIR results of the 7 days hydrated CM-RS mix distinctly showed the formation of M-S-H and its corresponding effect is clearly visible from the strength values. At later ages (28 days), the slower reacting SF continued to form M-S-H, resulting in an increase in strength. The difference in strength at 28 days between CM-SF and CM-RS mix is likely due to the difference in w/b ratio. The RM-RS mix also showed ~20% higher strength as compared to CM-SF mix at 3 days even with a 50% higher w/b ratio. The continual strength gain with age indicates continuous formation of hydration products. The strength development characteristics displayed by RM-RS mix validates the possibility of producing MgO-SiO<sub>2</sub> binder using magnesium silicate minerals.

The mechanical performance of the binder system was affected by the physical and chemical features of the raw materials and the mix design. The porosity of the mortar was not directly measured in this investigation due to the limited amount of recovered material. The similar spread values for the different mixes provides some indication of the workability but variations in w/b ratio will also

contribute to differences in the volume of capillary pores. Further work is necessary to accurately quantify both the fresh and hardened properties (including: porosity, permeability, resistivity) of the mortar or concrete. An improvement in the mechanical performance of the binder from recovered materials is likely with use of water-reducing admixtures, improved mixing, and improvement in the recovery process.

## Sustainability Assessment

The production of Portland cement typically requires approximately 3 GJ of energy and releases a total of 830 kg of CO<sub>2</sub>, per tonne of clinker for a modern kiln (Gartner and Sui 2018). The majority of the CO<sub>2</sub> is released from the calcination of limestone. In comparison the production of 1 tonne of MgO from olivine requires ~9.3 GJ/tonne, however every tonne of MgO is also accompanied by 1.27 tonnes of reactive silica. While a MgO:SiO<sub>2</sub> ratio of 1:1 was used in this work, Tran and Scott (2017) have shown effective binder systems can be produced with MgO:SiO<sub>2</sub> ratios from 0.4 to 0.6 for commercially available MgO, from magnesite, and silica fume. The energy demand for a binder using all of the recovered MgO and silica at a ratio of 0.44 would be ~4.1 GJ/tonne. While the total energy is higher for the MgO-silica binder system there is no chemical CO<sub>2</sub> produced in the manufacturing process. The CO<sub>2</sub> generated from the production of the binder therefore will depend upon the source of electricity. If green energy is used then the associated CO<sub>2</sub> is essentially zero. In a more realistic

situation where a mixed energy system is used such as California with ~50% fossil fuels and CO<sub>2</sub> emissions of 62.5 kg/GJ, the total CO<sub>2</sub> emissions for the MgO-SiO<sub>2</sub> binder are 255 kg/tonne, which is considerably less than that for Portland cement.

## CONCLUSION

This study investigated the hydration and microstructure features of MgO-SiO<sub>2</sub> binders produced using materials recovered from olivine. The characteristics of the binder produced were compared with binders made using commercially available materials. The major findings from the study can be summarized as follows:

- The recovered MgO and SiO<sub>2</sub> both showed a greater reactivity compared to commercial counterparts. The use of recovered silica in particular helped in enhancing the rate of hydration.
- The formation of M-S-H during hydration was confirmed in binder produced using the recovered materials.
- A comparable compressive strength performance of the CM-RS mix and CM-SF mix was observed. 28 days mortar strength in excess of 20 MPa were obtained with the recovered materials in the RM-RS mix.

The results confirm that it is possible to produce MgO-SiO<sub>2</sub> binders from magnesium silicate minerals with comparable results to more commonly available commercial materials.

## REFERENCES

- Abdel-Gawwad, H. A., Abd El-Aleem, S., Amer, A. A., El-Didamony, H., and Arif, M. A. (2018). Combined Impact of Silicate-Amorphicity and MgO-Reactivity on the Performance of Mg-Silicate Cement. *Construction Building Mater.* 189, 78–85. doi:10.1016/j.conbuildmat.2018.08.171
- ASTM C109 (2010). Standard Test Method for Compressive Strength of Hydraulic Cement Mortars (Using 2-in or 50mm Cube Specimens). *Am. Soc. Test. Mater.* 4, 1–9. doi:10.1520/C0109
- Bernard, E., Lothenbach, B., Chlique, C., Wyrzykowski, M., Dauzères, A., Pochard, I., et al. (2019). Characterization of Magnesium Silicate Hydrate (M-S-H). *Cement Concrete Res.* 116, 309–330. doi:10.1016/j.cemconres.2018.09.007
- Bernard, E., Lothenbach, B., Le Goff, F., Pochard, I., and Dauzères, A. (2017). Effect of Magnesium on Calcium Silicate Hydrate (C-S-H). *Cement Concrete Res.* 97, 61–72. doi:10.1016/j.cemconres.2017.03.012
- Besbes, M., Fakhfakh, N., and Benzina, M. (2009). Characterization of Silica Gel Prepared by Using Sol-Gel Process. *Phys. Proced.* 2, 1087–1095. doi:10.1016/j.phpro.2009.11.067
- Bhagath Singh, G. V. P., Sonat, C., Yang, E. H., and Unluer, C. (2020). Performance of MgO and MgO-SiO<sub>2</sub> Systems Containing Seeds under Different Curing Conditions. *Cement and Concrete Composites* 108, 103543. doi:10.1016/j.cemconcomp.2020.103543
- Brew, D. R. M., and Glasser, F. P. (2005). Synthesis and Characterisation of Magnesium Silicate Hydrate Gels. *Cement Concrete Res.* 35, 85–98. doi:10.1016/j.cemconres.2004.06.022
- Dhakal, M., Scott, A. N., Shah, V., Dhakal, R. P., and Clucas, D. (2021). Development of a MgO-Metakaolin Binder System. *Construction Building Mater.* 284, 122736. doi:10.1016/j.conbuildmat.2021.122736
- Gartner, E., and Sui, T. (2018). Alternative Cement Clinkers. *Cement Concrete Res.* 114, 27–39. doi:10.1016/j.cemconres.2017.02.002

## DATA AVAILABILITY STATEMENT

The raw data supporting the conclusions of this article will be made available by the authors, without undue reservation.

## AUTHOR CONTRIBUTIONS

VS: Conceptualization; Methodology; Data Curation; Formal Analysis; Investigation; Writing-original draft, AS: Conceptualization; Methodology; Resources; Formal Analysis, Funding Acquisition, Writing-review and editing, CO: Conceptualization; Writing-review and editing, BS: Investigation; Methodology; Data Curation, CC: Writing-review and editing.

## FUNDING

Financial support provided by the Ministry of Business, Innovation and Employment, New Zealand for this project.

## ACKNOWLEDGMENTS

The authors would also like to acknowledge the financial support provided by the Ministry of Business, Innovation, and Employment, New Zealand (1708) to this project.

- Gorrepati, E. A., Wongthahan, P., Raha, S., and Fogler, H. S. (2010). Silica Precipitation in Acidic Solutions: Mechanism, pH Effect, and Salt Effect. *Langmuir* 26, 10467–10474. doi:10.1021/la904685x
- Jia, Y., Wang, B., Wu, Z., and Zhang, T. (2017). Effect of CaO on the Reaction Process of MgO-SiO<sub>2</sub>-H<sub>2</sub>O Cement Pastes. *Mater. Lett.* 192, 48–51. doi:10.1016/j.matlet.2017.01.072
- Jin, F., and Al-Tabbaa, A. (2014). Strength and Hydration Products of Reactive MgO-Silica Pastes. *Cem. Conc. Comp.* 52, 27–33. doi:10.1016/j.cemconcomp.2014.04.003
- Kajaste, R., and Hurme, M. (2016). Cement Industry Greenhouse Gas Emissions - Management Options and Abatement Cost. *J. Clean. Prod.* 112, 4041–4052. doi:10.1016/j.jclepro.2015.07.055
- Katouezadeh, E., Rasouli, M., and Zebarjad, S. M. (2020). A Comprehensive Study on the Gelation Process of Silica Gels from Sodium Silicate. *J. Mater. Res. Techn.* 9, 10157–10165. doi:10.1016/j.jmrt.2020.07.020
- Li, Z., Xu, Y., Zhang, T., Hu, J., Wei, J., and Yu, Q. (2018). Effect of MgO Calcination Temperature on the Reaction Products and Kinetics of MgO-SiO<sub>2</sub>-H<sub>2</sub>O System. *J. Am. Ceram. Soc.* 102, 3269–3285. doi:10.1111/jace.16201
- Lieftink, D. J., and Geus, J. W. (1998). The Preparation of Silica from the Olivine Process and its Possible Use as a Catalyst Support. *J. Geochemical Exploration* 62, 347–350. doi:10.1016/S0375-6742(97)00067-8
- Matter, J. M., and Kelemen, P. B. (2009). Permanent Storage of Carbon Dioxide in Geological Reservoirs by Mineral Carbonation. *Nat. Geosci* 2, 837–841. doi:10.1038/ngeo683
- Pacheco-Torgal, F. Shi, C., and Palomo, A. (2018). *Carbon Dioxide Sequestration in Cementitious Construction Materials*. Duxford, United Kingdom: Woodhead. doi:10.1016/B978-0-08-102444-7.00007-1
- Rahman, I. A., and Padavettan, V. (2012). Synthesis of Silica Nanoparticles by Sol-Gel: Size-Dependent Properties, Surface Modification, and Applications in Silica-Polymer Nanocomposites-A Review. *J. Nanomater.* 2012, 1–15. doi:10.1155/2012/132424
- Raza, N., Raza, W., Madeddu, S., Agbe, H., Kumar, R. V., and Kim, K.-H. (2018). Synthesis and Characterization of Amorphous Precipitated Silica from Alkaline Dissolution of Olivine. *RSC Adv.* 8, 32651–32658. doi:10.1039/c8ra06257a

- Sanna, A., Lacinska, A., Styles, M., and Maroto-Valer, M. M. (2014). Silicate Rock Dissolution by Ammonium Bisulphate for pH Swing Mineral CO<sub>2</sub> Sequestration. *Fuel Process. Techn.* 120, 128–135. doi:10.1016/j.fuproc.2013.12.012
- Sanna, A., Wang, X., Lacinska, A., Styles, M., Paulson, T., and Maroto-Valer, M. M. (2013). Enhancing Mg Extraction from Lizardite-Rich Serpentine for CO<sub>2</sub> Mineral Sequestration. *Minerals Eng.* 49, 135–144. doi:10.1016/j.mineng.2013.05.018
- Scott, A., Oze, C., Shah, V., Yang, N., Shanks, B., Cheeseman, C., et al. (2021). Transformation of Abundant Magnesium Silicate Minerals for Enhanced CO<sub>2</sub> Sequestration. *Commun. Earth Environ.* 2, 1–6. doi:10.1038/s43247-021-00099-6
- Shah, V., and Scott, A. (2021a). Assessment of the Hardened Concrete Properties of MgO-SiO<sub>2</sub> Binder. *ACI Mater. J.* 118, 223–232. doi:10.14359/51730418
- Shah, V., and Scott, A. (2019). Use of Kaolin Clay as a Source of Silica in MgO-SiO<sub>2</sub> Binder. *Calcined Clays for Sustainable Concrete.* 815–819. doi:10.1007/978-981-15-2806-4\_91
- Shah, V., and Scott, A. (2021b). Use of Kaolinite Clays in Development of a Low Carbon MgO-Clay Binder System. *Cement Concrete Res.* 144, 106422. doi:10.1016/j.cemconres.2021.106422
- Shand, M. A. (2006). *The Chemistry and Technology of Magnesia*. Hoboken, NJ: John Wiley & Sons, Inc. doi:10.1002/0471980579
- Sonat, C., and Unluer, C. (2019). Development of Magnesium-Silicate-Hydrate (M-S-H) Cement with Rice Husk Ash. *J. Clean. Prod.* 211, 787–803. doi:10.1016/j.jclepro.2018.11.246
- Tonelli, M., Martini, F., Calucci, L., Fratini, E., Geppi, M., Ridi, F., et al. (2016). Structural Characterization of Magnesium Silicate Hydrate: Towards the Design of Eco-Sustainable Cements. *Dalton Trans.* 45, 3294–3304. doi:10.1039/c5dt03545g
- Tran, H. (2019). *Development of Magnesium Silicate Hydrate Binder Systems*. Christchurch, New Zealand: University of Canterbury. doi:10.1287/de028372-ab5d-470f-af4c-1bf36788a130
- Tran, H. M., and Scott, A. (2017). Strength and Workability of Magnesium Silicate Hydrate Binder Systems. *Construction Building Mater.* 131, 526–535. doi:10.1016/j.conbuildmat.2016.11.109
- UN Environment, Scrivener, K. L., John, V. M., and Gartner, E. M. (2018). Eco-efficient Cements: Potential, Economically Viable Solutions for a low-CO<sub>2</sub> Cement Based Industry. *Cem. Concr. Res.* 114, 64.
- Vandeperre, L. J., Liska, M., and Al-Tabbaa, A. (2008). Hydration and Mechanical Properties of Magnesia, Pulverized Fuel Ash, and Portland Cement Blends. *J. Mater. Civ. Eng.* 20, 375–383. doi:10.1061/(asce)0899-1561(2008)20:5(375)
- Vlasopoulos, N., and Cheeseman, C. R. (2013). *Binder Compositoin*, 2.
- Walling, S. A., Kinoshita, H., Bernal, S. A., Collier, N. C., and Provis, J. L. (2015). Structure and Properties of Binder Gels Formed in the System Mg(OH)<sub>2</sub>-SiO<sub>2</sub>-H<sub>2</sub>O for Immobilisation of Magnox Sludge. *Dalton Trans.* 44, 8126–8137. doi:10.1039/c5dt00877h
- Walling, S. A., and Provis, J. L. (2016). Magnesia-based Cements: A Journey of 150 years, and Cements for the Future? *Chem. Rev.* 116, 4170–4204. doi:10.1021/acs.chemrev.5b00463
- Zhang, T., Cheeseman, C. R., and Vandeperre, L. J. (2011). Development of Low pH Cement Systems Forming Magnesium Silicate Hydrate (M-S-H). *Cement Concrete Res.* 41, 439–442. doi:10.1016/j.cemconres.2011.01.016
- Zhang, T., Vandeperre, L. J., and Cheeseman, C. R. (2014). Formation of Magnesium Silicate Hydrate (M-S-H) Cement Pastes Using Sodium Hexametaphosphate. *Cement Concrete Res.* 65, 8–14. doi:10.1016/j.cemconres.2014.07.001
- Zhang, T., Vandeperre, L. J., and Cheeseman, C. R. (2012). Magnesium-silicate-hydrate Cements for Encapsulating Problematic Aluminium Containing Wastes. *J. Sust. Cement-Based Mater.* 1, 34–45. doi:10.1080/21650373.2012.727322
- Zhang, T., Zou, J., Wang, B., Wu, Z., Jia, Y., and Cheeseman, C. (2018). Characterization of Magnesium Silicate Hydrate (MSH) Gel Formed by Reacting MgO and Silica Fume. *Materials* 11, 909–915. doi:10.3390/ma11060909

**Conflict of Interest:** The authors declare that the research was conducted in the absence of any commercial or financial relationships that could be construed as a potential conflict of interest.

Copyright © 2021 Allan Nye, Vineet, Christopher, Barnaby and Chris. This is an open-access article distributed under the terms of the Creative Commons Attribution License (CC BY). The use, distribution or reproduction in other forums is permitted, provided the original author(s) and the copyright owner(s) are credited and that the original publication in this journal is cited, in accordance with accepted academic practice. No use, distribution or reproduction is permitted which does not comply with these terms.